

Spring 5-18-2012

Design and Testing of the Measuring System for the Characterization of Magnetoelectric Composites

Thomas S. Ward IV
University of New Orleans

Follow this and additional works at: <https://scholarworks.uno.edu/td>



Part of the [Physics Commons](#)

Recommended Citation

Ward, Thomas S. IV, "Design and Testing of the Measuring System for the Characterization of Magnetoelectric Composites" (2012). *University of New Orleans Theses and Dissertations*. 1495.
<https://scholarworks.uno.edu/td/1495>

This Thesis is protected by copyright and/or related rights. It has been brought to you by ScholarWorks@UNO with permission from the rights-holder(s). You are free to use this Thesis in any way that is permitted by the copyright and related rights legislation that applies to your use. For other uses you need to obtain permission from the rights-holder(s) directly, unless additional rights are indicated by a Creative Commons license in the record and/or on the work itself.

This Thesis has been accepted for inclusion in University of New Orleans Theses and Dissertations by an authorized administrator of ScholarWorks@UNO. For more information, please contact scholarworks@uno.edu.

Design and Testing of the Measuring System for the Characterization of
Magnetoelectric Composites

A Thesis

Submitted to the Graduate Faculty of the
University Of New Orleans
in partial fulfillment of the
requirements for the degree of

Master of Science
in
Applied Physics

By
Thomas Ward
B.S. Roanoke College, 2007
May 2012

ACKNOWLEDGEMENT

I wish to sincerely thank my family for their support and motivation. I would also like to thank Kelly Ann Leilich for everything she has done in this process. Sincere thanks goes to Dr. Stokes and his group for the assistance in hot pressing samples early on in my research and the use of his lock-in amplifier. I would also like to express my appreciation to Dr. Spinu for allowing my use of the Gaussmeter in the calibration of my coil as well as other equipment his group assisted me in using early on in my graduate career. Also, I would extend my gratitude to the Physics Department for giving me the opportunity to pursue this degree and AMRI for allowing me to have a research position. Finally, thanks to my research group and advisor Dr. Leszek Malkinski. Without their guidance and help this would not have been possible.

TABLE OF CONTENTS

List of Figures.....	v
Abstract.....	vii
Chapter 1 Introduction.....	1
Chapter 2 Theory	3
Chapter 2.1 Magnetostriction and Piezomagnetism	3
Chapter 2.2 Piezoelectricity	5
Chapter 2.3 Resonance and Mechanical Factors.....	7
Chapter 2.4 Magnetoelectric Effect	11
Chapter 3 Experiment.....	15
Chapter 3.1 Fabrication of the Measurement System.....	15
Chapter 3.2 Samples	24
Chapter 4 Procedures and Results	26
Chapter 4.1 Magnetic and Electric Properties Characterization	26
Chapter 4.2 Magnetomechanical Resonance	31
Chapter 4.3 Electromechanical Resonance	34
Chapter 4.4 Magnetoelectrical Properties- Direct Effect.....	36
Chapter 4.5 Magnetoelectric Effect- Converse Direct	38
Chapter 5 Conclusions	45
References	49
Vita.....	51

List of Figures

Figure 1: Magnetic domain wall orientations	4
Figure 2: Resonance Peak Example.....	6
Figure 3: Magnetomechanical resonance of a magnetostrictive sample when vibrations are excited by magnetic field with varying frequency	10
Figure 4: Diagram of Magnetoelectric Effect and Converse Magnetoelectric effect ...	12
Figure 5: Magnetic Measurements Connections Schematic	15
Figure 6: Electric Measurements Configuration	16
Figure 7: Picture of the Fabricated System.....	16
Figure 8: Magnetic moment alignment due to a field	17
Figure 9: Measured fields generated by the bias coil	19
Figure 10: Resonance Frequency Sweep of FeSiB/AIN	27
Figure 11: Resonance Test Configuration FeSiB	26
Figure 12: Relative permeability as a function of bias field for FeSiB/PZT	29
Figure 13: PZT Hysteresis loop from "Correlation between local hysteresis and crystallite orientation in PZT thin films deposited on Si and MgO Substrates."	30
Figure 14: Resonance Sweep of FeSiB Amorphous Ribbon showing relative permeability versus Frequency	32
Figure 15: Configuration for exclusively electric data results.....	35
Figure 16: Electromechanical resonance sweep	35
Figure 17: Measured Impedance with frequency dependence subtracted	34
Figure 18: Schematic for electric displacement due to ΔH system connections.....	37
Figure 19: Magnetic field frequency versus change in electric displacement signal ..	38
Figure 20: General configuration for electric resonance sweep	39
Figure 21: Resonance frequency scan for the applied E field of PZT showing α^T	40
Figure 22: Measured change in B comparison due to E and frequency.....	41
Figure 23: Signal varying due to bias field sweeps	42
Figure 24: Ratio of response as a result of amplitude variation	44
Table 1A: Lists of possible measurements.....	48
Table 1B: Lists of possible measurements continued	49

Abstract

The goal of this thesis is to design, build and test a new measurement system for comprehensive studies of the magnetoelectric and the converse magnetoelectric effect. The research on multiferroic composites is an emerging field of research and there is no commercially available equipment. The method proposed here for testing magnetoelectric properties of the multiferroics is relatively inexpensive and versatile. The advantage of the new method described below is that the same set of instruments in different configurations enables multiple measurements of various parameters characterizing multiferroic composites.

The system was tested using two samples $\text{Fe}_{78}\text{Si}_{10}\text{B}_{12}/\text{AlN}$ and $\text{Fe}_{78}\text{Si}_{10}\text{B}_{12}/\text{PZT}$ consisting of ferromagnetic and magnetostrictive ribbon of metallic glass glued to piezoelectric AlN or PZT. The final result was a working system that enables selective measurements of different responses of the multiferroic composites to the static and dynamic electric and magnetic fields. This demonstrates the versatility of the system.

Magnetoelectrical effect, Piezoelectric, Piezomagnetic, magneticmechanical, electromechanical, magnetoelectrical measurement

Chapter 1

Introduction

This thesis is to outline and document the invention of a versatile method to test the magnetoelectric effect as well as the converse magneto-electric effect in multiferroic materials. Multiferroic materials exhibit both ferroelectric and ferromagnetic properties which are mutually coupled. There are only few known single phase materials which show weak coupling between magnetism and ferroelectricity (usually below room temperature). However, much stronger coupling has been found in multiferroic composites, where the stresses due to piezoelectric or magnetostrictive properties mediate the process of exchange of energy. The magnetoelectric effect manifests itself when an alternating current field is applied to the sample as well as a small direct current bias field. A more in-depth discussion of this will come about in a later section as a detailed description of the system.

The purpose of the system, that was built, was to test both magnetic and electric properties as well as the coupling between them. In some labs you have equipment that can take readings regarding either one set of properties or the other. The system that was fabricated allows for selective testing of different components of the equations describing multiferroic composites by varying connections within the same system.

A secondary advantage to the fabrication of this system was its cost. Most systems in research today have price tags of over \$100,000 which may not be an option. This system was fabricated for a fraction of that cost using common instrumentation. The main cost will be a function generator with two channels, a lock-in amplifier, copper wire, and two power supplies. Granted, some of these items are not particularly cheap, however, the total cost will still be minimal in comparison to other equipment.

Finally, this system will be able to handle bulk composites samples. While some equipment must have a minimal sample to fit, this system will allow for larger sizes. Also, solenoid coils can be fabricated to facilitate various sample size, thus making the system more accommodating of various geometries.

Chapter 2

Theory

2.1 Magnetostriction and Piezomagnetism:

Many magnetic materials exhibit a mutual coupling between magnetic and elastic properties. Magnetostriction is determined as the change of materials' physical dimensions (linear dimensions, shape or volume) due to a change to the materials' magnetization. In particular, in case of linear dimensions the relative change of dimensions measured along the direction of the applied magnetic field H defines linear magnetostriction:

$$\lambda(H) = \Delta l / l. \quad (1)$$

Here l is the length of the sample in demagnetized state and Δl is the magnetostrictive strain. Saturation magnetostriction coefficient λ_s corresponds to a maximum relative change of length between demagnetized state and technical magnetic saturation. This is usually what is meant when the term magnetostriction is used unless previously qualified. [1] The microscopic origin of magnetostriction is the coupling between spin and orbital motion of electrons [2]. Macroscopic samples consist of many domains- volumes with uniformly aligned and coupled (through quantum exchange interaction) magnetic moments which are separated by domain walls. Deformation of the macroscopic samples can be explained by

rearrangement of domain structure which occurs through domain magnetization rotations or domain wall displacements. This mechanism of magnetostriction is illustrated in Fig.1.

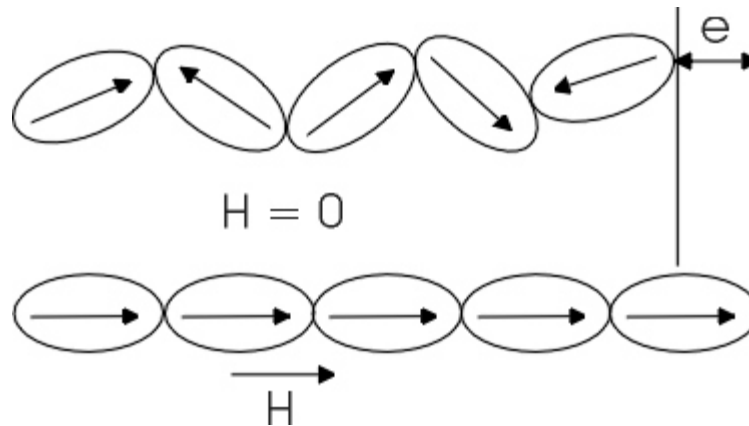


Figure 1: Magnetic domain wall orientations

<http://aml.seas.ucla.edu/research/areas/magnetostrictive/mag-composites/Magnetostriction%20and%20Magnetostrictive%20Materials.htm>

A material can be made up of multiple domains that at any time could have random orientation when $H=0$. As H is increased the magnetization vectors of domains will rotate to align themselves with applied field (H) orientation. When all the magnetic domains are aligned in the same direction the sample is considered saturated. At this point the samples physical deformation will be at its greatest. The process of reorientation of the domain structure in a magnetic field is usually nonlinear, and consequently the relation between the magnetostriction and field is determined by nonlinear function [3]. However, for small changes of magnetic field the magnetostrictive strains are proportional to the field. This is called a piezomagnetic limit.

This effect can also work in a converse manner, which means that the magnetization can be changed by deforming material or applying stresses.

The linear piezomagnetic equations which describe mutual relation between strain S and stress T components and magnetic induction B or field H components can be written as follows:

$$S_i = s_{ij}^H T_j + q_{ij} H_j \quad (2)$$

$$B_i = \mu_{ij}^T H_j + q_{ij} S_j \quad (3)$$

Here, s_{ij} is the mechanical compliance tensor measured at constant field, μ is the permeability tensor at constant stress and q is the piezomagnetic coefficient tensor.

2.2 Piezoelectricity:

Piezoelectricity is where electrical and mechanical energies can be directly converted from one to the other. These materials produce an electric charge when a mechanical stress is applied. This is called the “direct effect.” In contrast when an electric field is applied the material experiences a stress thus causing a mechanical deformation happen. When this situation occurs it is dubbed the “converse effect.” The origin of the piezoelectricity is asymmetric crystal structure of the materials, where positive and negative ions in their unit cells are displaced with respect to each other. The strains applied to the material can polarize or change already existing permanent

polarization by varying the distance between the ions. Both of these effects can happen in both single crystal and polycrystalline structures. Some piezoelectrics are ferroelectric, which means that they have permanent polarization. Macroscopic samples consist of many domains- regions with uniform polarization which are separated by domain walls which can displace in the presence of applied electric field. To maximize the piezoelectric effect the poling of a polycrystalline sample is needed. This will align almost all the moments of ferroelectric domains in the same direction to negate anisotropy.

Mathematical equations have been derived to explain this effect. The piezoelectric equations for small applied electric field and small stresses have similar form to the piezomagnetic equations:

$$S_i = s_{ij}^E T_j + d_{ij} E_j \quad (4)$$

$$D_i = \epsilon_{ij}^T E_j + d_{ij} T_j \quad (5)$$

In these two equations S is the mechanical strain and D is the electric displacement. The variable T represents the mechanical stress while E is the electric field. The elastic compliance is denoted as s -tensor and ϵ represents electric permittivity tensor (dielectric constant), while d and the piezoelectric constant tensor [4]. In these equations the superscripts mean either a constant stress for T or constant electric field denoted by E . [5]

There are two ways to derive the piezoelectric constant. The piezoelectric constant is symbolized by d . The first way is if you measure certain component of mechanical strain generated by the application of an electric field in specific direction. This can be shown as:

$$d = \frac{\text{strain development}}{\text{applied electric field}} \quad (6)$$

Next would be the measuring the electric displacement due to known mechanical stress applied. The equation is:

$$d = \frac{\text{short circuit charge density}}{\text{applied mechanical stress}} \quad (7)$$

In both methods of equations above the piezoelectric constant is used for the final calculation of strain or displacement due to the piezoelectric effect [6].

2.3 Resonance and Mechanical Factors:

This section will discuss the mechanical factors that go into this experiment. The first major factor is resonance. At resonance we will achieve the maximum amplitude of oscillations of our samples. Resonance is the result of a certain frequency at which the wavelength matches certain dimensions of the vibrating sample. This equates to the maximum signal that will register on the lock-in amplifier [7]. Equations can be set up to derive and explain this phenomenon. First, take ω_R to be the resonant frequency and A

to be amplitude. Next the equation for amplitude in relation to oscillations is found to be:

$$A = \frac{A_0}{\sqrt{(\omega_0^2 - \omega^2) + 4\omega^2\beta^2}} \quad (8)$$

In the previous equation ω represents the angular frequency. The β term is the damping parameter. As can be seen in the previous equation if you have minimum damping the second term becomes very small. This allows for the potential of achieving greater amplitude. Then it can also be noted that when ω and ω_0 are close this will cause the amplitude to be greater. Conversely, if the two frequencies are set to be far apart then the achieved amplitude will be much smaller. Knowing this a differentiation can be done to find the resonant frequency.

$$\frac{dA}{d\omega} = 0 \rightarrow \omega = \omega_R \quad (9)$$

And the resultant resonant frequency can be written as:

$$\omega_R = \sqrt{\omega_0^2 - 2\beta^2} \quad (10)$$

This equation represents resonant frequency with damping factored in [8]. When the conditions are set to achieve the frequency ω_R the response will be at its maximum [9]. In addition to the damping resulting from materials properties there is additional damping expected in our samples due to the leads and surface interactions. A resultant graph of a frequency sweep can

be plotted that shows what is derived above to be true. In the following graph it can be seen when the natural frequency and driving frequency are the same you achieve a maximum response.

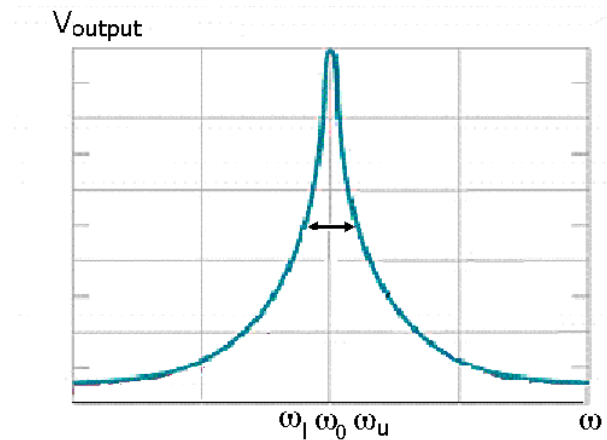


Figure 2: Resonance Peak Example

<http://www.insula.com.au/physics/1221/L1 1>

Damping also can be seen in the graph. The width of the peak is reliant on the damping coefficient. The smaller your β the sharper and narrower your resonant peak will appear. At the two points on the curve at exactly half the maximum height you can measure the width. This width equates to approximately 2β . In knowing this the β term can be calculated to show what damping constant is present in the sample [10].

The graph in Fig. 2 shows typical mechanical resonance curve of materials which are neither piezoelectric nor magnetostrictive. The vibrations of the magnetostrictive samples can be excited by alternating magnetic field which

produces periodic strains in the sample. The example of the resonant curve for magnetostrictive sample which represents magnetomechanical resonance is presented in Fig. 3.

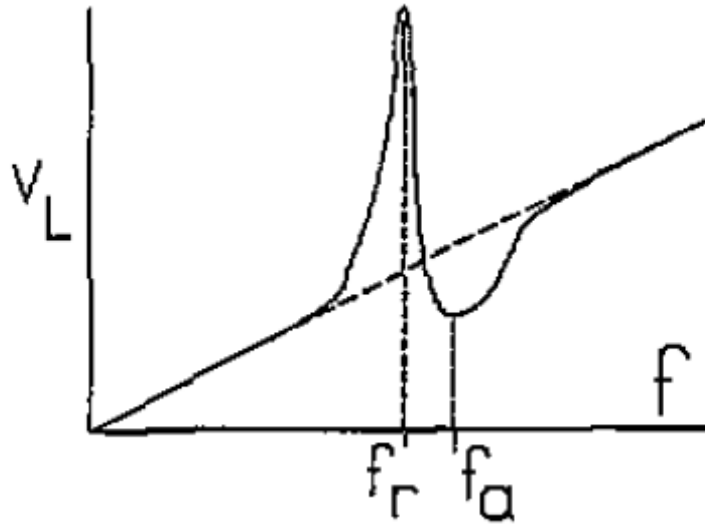


Fig.3. Magnetomechanical resonance of a magnetostrictive sample when vibrations are excited by magnetic field with varying frequency. [11]

The resonant f_r and antiresonant f_a frequencies can be used to calculate the magnetomechanical coupling factor k which describes the ratio of the energy of magnetic field which is converted into energy of mechanical vibrations.

The formula for the magnetomechanical factor k_H for the longitudinal samples is as follows:

$$k_H = \frac{\pi}{2} \sqrt{\frac{f_a^2 - f_r^2}{2f_a^2}} \quad (11)$$

Similar resonance curves can be plotted for the piezoelectric samples in which resonant vibrations are excited by the alternating electric field due to their piezoelectric strains. In the case of electromechanical resonance we can measure electromechanical coupling factor k_E , which determines the fraction of the electric field energy which is converted into mechanical energy of vibrations.

2.4 Magnetoelectric effect:

The simplest definition of the magnetoelectric effect is the coupling of electric and magnetic fields in matter. [12] Materials that exhibit the largest effect are usually composites. These composites consist of a piezoelectric material as well as a magnetostrictive material. The magnetoelectric effect was discovered in the late 1800's (it was first predicted by Curie in 1894) but only over the past decade it has gained popularity and a lot of research has gone into it [13, 14]. There has been an evolution of samples that are prepared and tested. To start there were single phase materials. These were followed by two phase bulk composites. Finally, multi-phase laminates were produced and tested. These laminates could have multiple phase materials layered on top of each other by various methods such as thin film deposition or adhesives to name a few. [15]

In these composites there are multiple components. First, there are ferroelectric materials with good piezoelectric parameters. This material can

be spontaneously polarized (in the case of poled PZT), although some piezoelectrics, such as AlN, are not ferroelectric and do not possess spontaneous polarization. For the purposes of this research the piezoelectrics will be a singular layer of our laminate composite sample. The second layer of the laminated structure is an amorphous ribbon with excellent magnetostrictive properties. The mechanism which links magnetic and electric properties of the two phases in the laminate composites is illustrated in Fig.4. Electric field produces strain in piezoelectric layer which strains the magnetostrictive layer and this produces change of magnetization (or induction) of the magnetic component. On the other hand, the magnetostrictive strain due to applied stress can be transferred to the piezoelectric layer and cause change of polarization (or electric displacement) as depicted in the bottom part of figure 4.

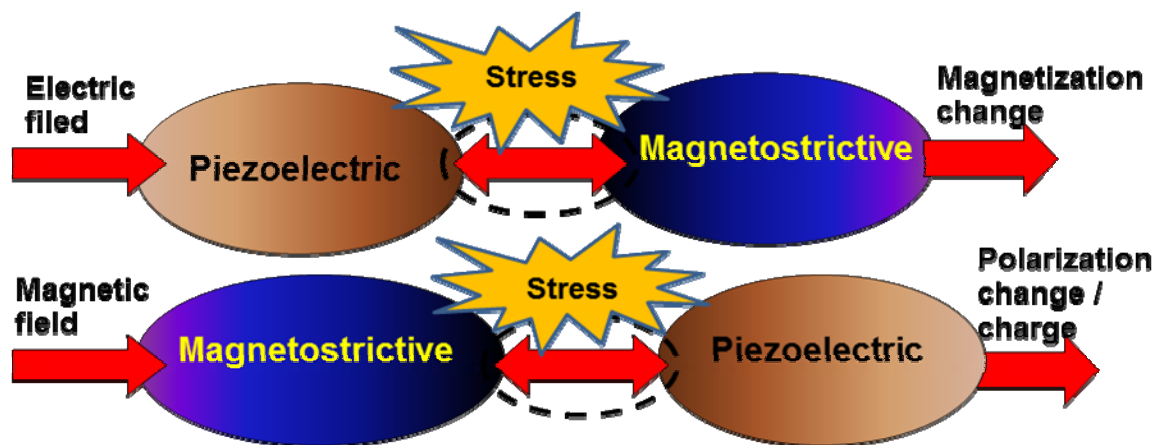


Figure 4: Diagram of Magnetoelectric Effect and Converse Magnetoelectric effect

The properties of these composite samples can be described by the set of equations which bind various components of electric and magnetic fields with electric displacement and magnetic induction vectors as well as strains and stresses. These equations are an expansion of piezoelectric and piezomagnetic equations (3 and 5) which include a magnetoelectric tensor.

$$D_i = \varepsilon_{ij}^T E_j + d_{ij} T_j + \alpha_{ij} H_j \quad (12)$$

$$B_i = \mu_{ij}^T H_j + q_{ij} S_j + \alpha_{ij}^* E_j \quad (13)$$

where magnetoelectric coefficients (α_{ij}) and transposed coefficients marked with * depend on piezoelectric (d_{ij}) and piezomagnetic (q_{ij}) coefficients but also on the quality of mechanical coupling between the two phases of the composite.

In the case of isotropic polycrystalline materials and for specific direction of the electric and magnetic fields the number of equations which describe the properties of multiferroics can be greatly reduced to scalar equations:

$$D = \varepsilon E + dT + \alpha H \quad (14)$$

$$B = \mu H + qS + \alpha^* E \quad (15)$$

In these equations D and B are measured along the uniaxial fields E , H . Next d , μ , q , and α are respectively the piezoelectric coefficient, permittivity (or

dielectric constant), piezomagnetic coefficient and magnetoelectric coefficient [16].

If there is a large damping coefficient tweaking the bonding methods or sample fabrication procedure might be required to elicit the maximum response. In preparation of the samples there are two different types of material coupled. Sample preparation may affect the interaction between the materials.

Chapter 3 Experiment

3.1 Fabrication of the Measurement System

The idea behind this experiment was to fabricate a system to measure both magnetomechanical and electromechanical coupling factors. Solenoid coils were the base of the design along with a few other electronics. The largest coil was made to generate a direct current magnetic bias field. The second coil received a signal from a function generator producing an alternating magnetic field that would be the driving coil of the system. This coil was used to measure differential permeability and to excite vibrations (at resonant frequency). Then the final coil(s) were the pickup and compensating coil which measured longitudinal (or along the applied bias field) change of magnetic flux. These two coils were in line and identical other than being wound in opposite directions. The following diagrams are a graphical representation of the system with two configurations that were used where every coil and piece of equipment is being used:

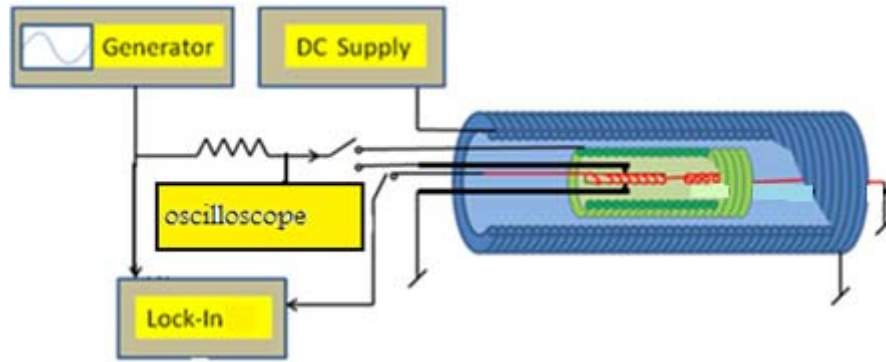


Figure 5: Magnetic Measurements Connections Schematic

The system in figure 5 is used in taking magnetic measurements. It has more coils than the system in figure 6 to measure voltage or changes of the impedance of the piezoelement due to magnetic field.

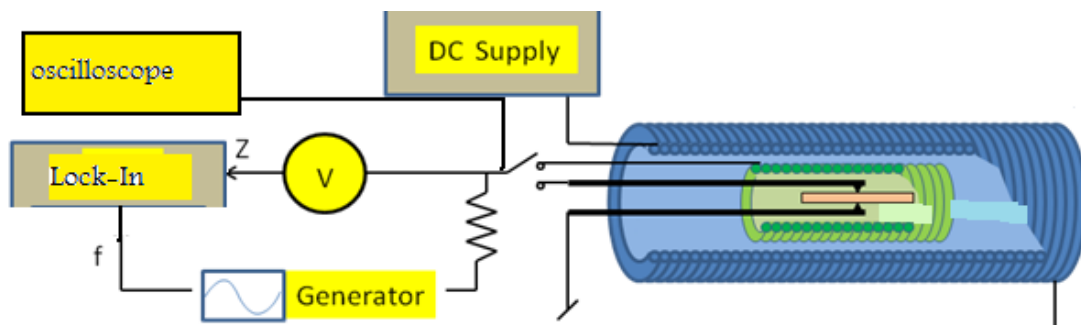


Figure 6: Electric Measurements Configuration

The system in figure 6 is used for taking electric measurements. This system takes the response straight from leads attached to the sample. The final product in Fig.7 looks like the picture below to present a non-schematic view.



Figure 7: Picture of the Fabricated System

Demagnetized multidomain samples or magnetically saturated samples do not change their dimensions in small ac magnetic fields. Therefore, it is necessary to use dc bias field to optimize magnetoelastic response of the samples, which is maximum for certain configuration of domain structure as pointed in Fig 8. The bias field generated by the outer coil serves the purposes of partial aligning the magnetic moments of the sample.

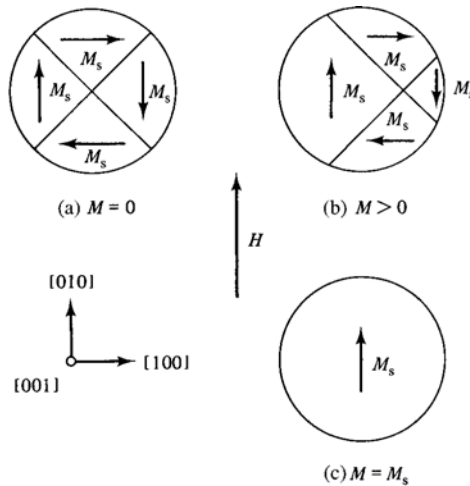


Figure 8: Magnetic moment alignment due to a field

INTRODUCTION TO MAGNETIC MATERIALS, B.D. Cullity, p.200

This solenoid coil was fabricated using flat copper 15 gauge wire. The ratio was 1:2 thicknesses to width. Multiple layers were wound over a length of Schedule 40 PVC pipe. There were 65 turns per 35 cm of length. Using this information Ampere's law comes in to define the magnetic field. This allows for simplification due to symmetry in contrast to using the Biot-Savart Law. [17] Ampere's law sets up the following equation for infinitely long solenoid:

$$H = n I \quad (11)$$

The components of this equation are H representing the magnetic field, n - the number of turns per unit length in the coil that the current I passes through [18]. The prior equation represents the magnetic field in the bias coil. After making the coil with four segments (layers) of wire that can be connected and or isolated on the solenoid there were measurements taken of the actual generated field for different positions along the length of the

coil using Lakeshore Gaussmeter with longitudinal Hall probe. These measurements were taken at a current of six (6) amps with the exception of the forth segment. The resistance in the coil made it only possible to achieve 4.84 amps at the maximum applied potential that the power supply could put out. Below is the graph of fields versus position. It shows good uniformity of the field in its central part. The power supply was maxed out for coil section four (4) making the resistance in the coil large enough so that a six ampere current could be reached. Instead at the maximum setting a current of 4.84 A was produced.

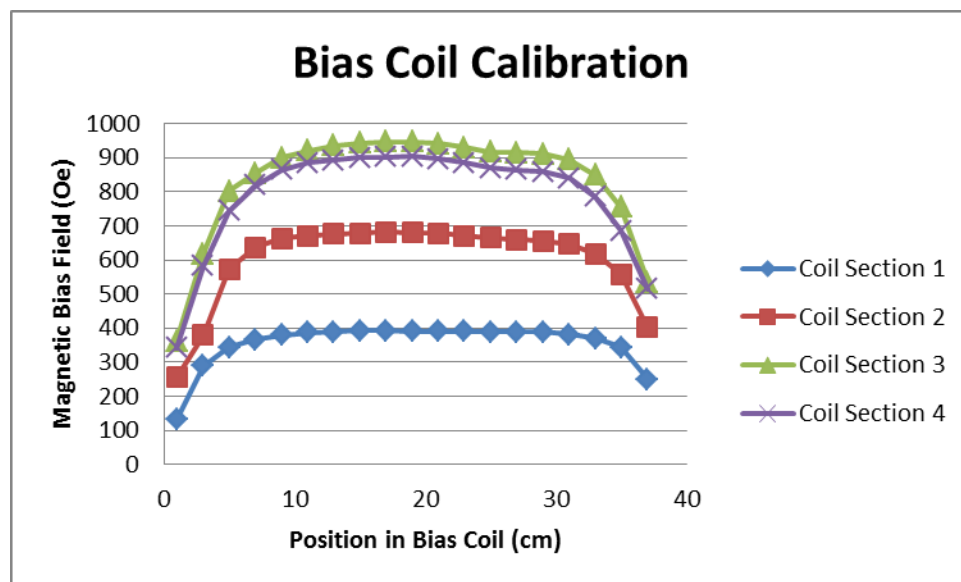


Figure 9: Measured fields generated by the bias coil

The next component is the driving coil. This coil is another solenoid coil wrapped with a single layer of insulated copper wire. This coil was made around a smaller piece of PVC pipe. The interior radius of the pipe measured 16.75 mm. There are 166 turns over the length of the solenoid. This coil fits directly inside is the driving coil. It uses an alternating current to

generate an alternating magnetic field. The amplitude of the sinusoidal ac magnetic field in the driving coil can be calculated based on Farady's law of induction using a pick up coil with known geometry and number of turns.

The equation is set up as such:

$$H = \frac{V}{n A 2 \pi f \mu_0} \quad (12)$$

In this equation H (in A/m) is induced magnetic field, v is the recorded amplitude of the signal in volts, n is the number of turns in the pickup coil, A is the cross sectional area of the coil (in m²), f is your set frequency in the driving coil (in Hz), and μ_0 is the permeability of a vacuum.

It is the intent of the driving coil to cause the orientation of the moments to rotate. The driving ac field can be used in two ways. For the frequencies far from the mechanical resonance ac excitations is used to measure magnetic permeability. This ac field will cause rotations of magnetization of domains and domain wall movements and thus a change in the flux in the pick-up coil. Since the changes of magnetization of the magnetostrictive sample are associated with the magnetoelastic strains in the sample, the same field at resonance can be used to excite significant longitudinal or flexural vibrations of the sample. In this case the whole purpose is to cause a change in the mechanical strain transferred to the piezoelectric material from the magnetostrictive.

The system is equipped with 2 coils: they are the pickup coil and compensating coil. Both the coils have magnetic flux generated by the driving coil passing through them. In this set up the compensating coil will be used to cancel out a signal generated by the driving coil. This allows the only signal to register in the pickup coil to be created by the sample loaded into the coil. Achieving this is done by having coils that are identical with the exception of windings going in opposite directions. The pickup coil will be wound clockwise with the compensating coil being wound in the counter clockwise direction. When a ferromagnetic sample with large permeability (compared to the permeability of free space) is inserted into the pick-p coil the signal from the two coils will no longer be balanced. Faraday's law of induction is the operating principle for these two coils. The following equation allows you to find the magnetic induction:

$$B = \frac{V}{n A_c 2 \pi f} \quad (13)$$

In this equation v is again the measured signal from the pickup coil, n is your number of turns in the driving coil per unit length and A_c is the cross sectional area of your sample. (Note that the air flux through the cross-sectional area of the pick-up coil is zero because of the use of compensating coil) . Next is the f which represents the frequency. The permeability can be calculated as the ratio of the B from equation (13) and H from equation (12) $\mu = \mu_0 \mu_r = B/H$, where μ_0 and μ_r are the permeability of vacuum and relative permeability, respectively.

Other equipment was used in this system in addition to just coils as can be seen in the prior schematics. There was a function generator from Agilent. This generator had two channels that could be tuned to different frequencies simultaneously. The generated signal could range from only a few milihertz to megahertz. Associated amplitudes for the signal generated by each channel could be set. These amplitudes ranged from millivolts up to ten volts peak-to-peak of a sinusoidal wave. Finally, you could set a phase difference if desired to tune the system using the function generator.

The next piece of equipment is the lock-in amplifier from Stanfrod Research Corporation. From this piece of equipment measurement data was displayed and recorded. Again, there was a phase shift dial for tuning the response signals to achieve the maximum reading. Multiple measurements could be made on the lock-in amplifier. Both, the transverse and longitudinal or x (which is the signal in-phase with the reference signal) and y (shifted in phase by $\pi/2$ with respect to the reference signal) components of the signal could be measured. Also, a measurement of the total magnitude of the signal could be made. This is able to be checked by the equation:

$$\text{Magnitude } R = \sqrt{x^2 + y^2} \quad (14)$$

Given this settings can be checked to make sure measurements are being made in the correct mode.

The two bipolar power supplies BOP76-6 from KEPCO were able to produce 76 volts with the frequency from DC to 20 kHz. These two power supplies

were used for bias or to amplify the signal from the generator. They were equipped with dials that allowed for smooth range sweeps that would assist in tuning the system. Given the ability to sweep the range smoothly it could be narrowed down to focus on certain smaller increments for the recorded data sets.

One power supply is used to supply the bias coil with a current. The ability to vary this current is critical in taking measurements. An amp meter was put in series with the coil to collect a more precise measurement of the dc current passing through the coil as this is part of the determining factors in the magnetic bias field.

The second power supply was used to bias the piezoelectric portion of the sample. In one configuration the generated signal from the function generator was passed through this power supply which would act as an amplifier. This allowed for the amplitude of the signal to be shifted or amplified.

Finally, an oscilloscope was used to monitor output signals on the sample (applied to the piezoelement) and on the driving coil. Also, a second channel was tied to the signal passing from the generator directly to the sample leads. This configuration allowed for confirmation that the signals being generated matched the settings on the function generator.

There were multiple configurations of these coils and pieces of equipment to isolate individual properties of a sample. As will be discussed in the

procedures section coils could be connected in multiple configurations to various pieces of equipment to generate different effects.

3.2 Samples:

The first sample that was used to achieve results was $\text{Fe}_{78}\text{Si}_{10}\text{B}_{12}/\text{PZT}$. The PZT was the piezoelectric material. In this sample the $\text{Fe}_{78}\text{Si}_{10}\text{B}_{12}$ ribbon was the magnetostrictive material. PZT is a piezoelectric with the largest known piezoelectric coefficient. Its composition is lead zirconate titanate. The $\text{Fe}_{78}\text{Si}_{10}\text{B}_{12}$ ribbon was made by rapid quenching of melt or more commonly called melt-spun. A rapid cooling of the melt at a rate of one million Kelvin per second does not allow for crystallization. Hence, the term amorphous or metallic glass when referring to this ribbon. The ribbon was then heat treated to maximize the magnetoelastic response. This sample was prepared by taking a ceramic plate of PZT and using an epoxy to attach the amorphous ribbon of $\text{Fe}_{78}\text{Si}_{10}\text{B}_{12}$. These two materials combined again formed a multiferrioc material. Silver paste was then used to attach wire leads to the sample that would assist in measurements and excitation of vibrations by the means of the ac electric field. This sample was used to perform all the required measurements.

The physical dimensions of this sample should be mentioned for later when the electric fields across the thickness of PZT and cross-sectional area of the amorphous ribbon must be known to calculate their properties. The

magnetostrictive ribbon composed of $\text{Fe}_{78}\text{Si}_{10}\text{B}_{12}$ has a width of 3.759 mm. The thickness of this ribbon was 18.9 micrometers. Finally, the length was 6.2 cm and density 7.16 G/cm. Next, the PZT sample is 6.284 mm wide and 0.355 mm thick.

There was a second sample used to show magneto mechanical resonance. The sample was made up of $\text{Fe}_{78}\text{Si}_{10}\text{B}_{10}/\text{AlN}$. In this sample the $\text{Fe}_{78}\text{Si}_{10}\text{B}_{10}$ was the magnetostrictive material. This material was then combined with epoxy to a plate of AlN. In this sample AlN was the piezoelectric material. Once these two were combined in the aforementioned manner they created a magnetoelectric composite. It should be noted that this plate was only attached to one side of the amorphous ribbon. Thus, any vibrations would cause the sample to bow causing a wave like motion with two nodes. Whichever material was not excited and was having the strain transferred to it would cause a slight clamping effect. There were no leads attached to this sample. The primary reason behind this sample was to do a preliminary trial run to see if resonance could be measured using our complete system.

Chapter 4

Procedures and Results

4.1 Magnetic and Electric Properties Characterization:

In this chapter procedures and results from that procedure will be discussed in an attempt to measure components that were mentioned before. The first test to see if a signal could be measured for a sample and if it could be then to determine if a resonance peak could be measured. For this initial test a sample consisting of $\text{Fe}_{78}\text{Si}_{10}\text{B}_{10}/\text{AlN}$ was used. Here a set up like figure 5 was used. No biasing field was applied. The function generator was set to deliver 10 volts peak to peak of a continuous sinusoidal signal to the driving coil. The frequencies were swept from 0 KHz to 100 KHz. A reading was recorded from the lock-in amplifier. Signals displayed on the lock-in were generated by the sample vibrating in the pickup coil. This coil registers the change in flux due to the sample, all external flux not related to the sample is canceled out by the compensating coil. The graph below is representative of what was achieved by recording the signal at multiple frequencies. You can see multiple peaks in this graph. These peaks are resonance peaks for the sample. The response was at resonance three separate times it appears. The sharpest and clearest peak is at a lower frequency. It is believed that

due to the samples design with only one side being laminated by an amorphous ribbon the sample was actually bending due to the magnetoelastic strain changes of the magnetostrictive ribbon. However, this proved that a signal could be generated by the system by excitation of the sample due to magnetic field. Also, this shows the magneto mechanical resonance which will be data that can be collected and used for calculations that will be demonstrated later in this section. The second peak corresponds to the longitudinal vibrations which will be studied for the other sample with PZT as the piezoelectric material. Finally, the broadest peak at about 90 kHz is due to the resonance of the inductive coils in the system.

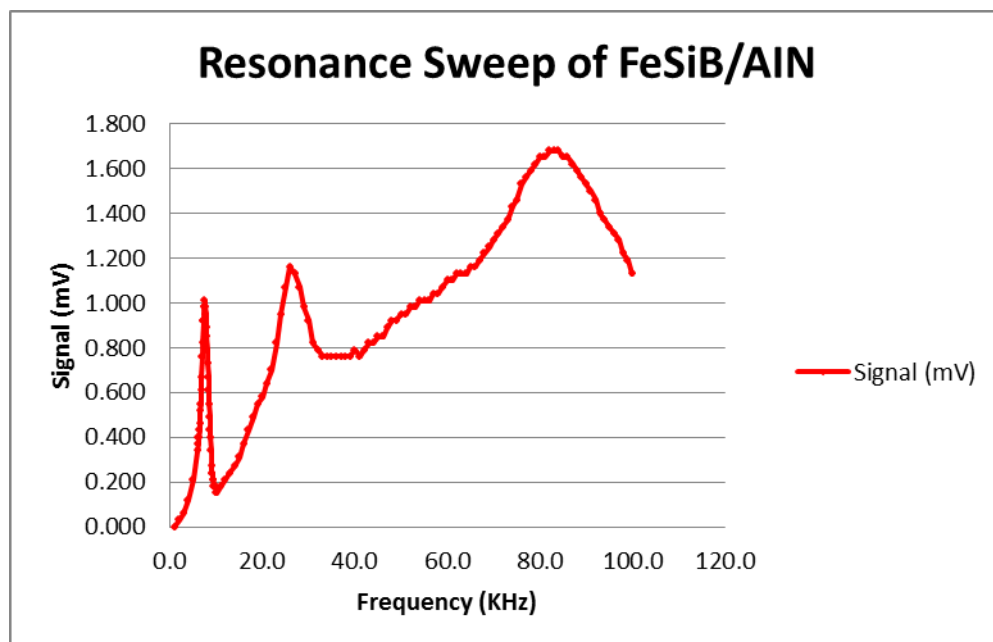


Figure 10: Resonance Frequency Sweep of FeSiB/AlN

Testing the second sample which was $\text{Fe}_{78}\text{Si}_{10}\text{B}_{12}/\text{PZT}$ was a multi step process. This sample was tested for both electric and magnetic qualities. Also, testing was done to demonstrate the coupling between phases. The first step was to test $\text{Fe}_{78}\text{Si}_{10}\text{B}_{12}$ amorphous ribbon by itself to establish its magnetic properties before attaching with epoxy to the ceramic PZT plate. Placing the amorphous ribbon in the pickup coil and then inserting the pickup coil into the driving coil which was already located in the bias coil. The following schematic represents the configuration.

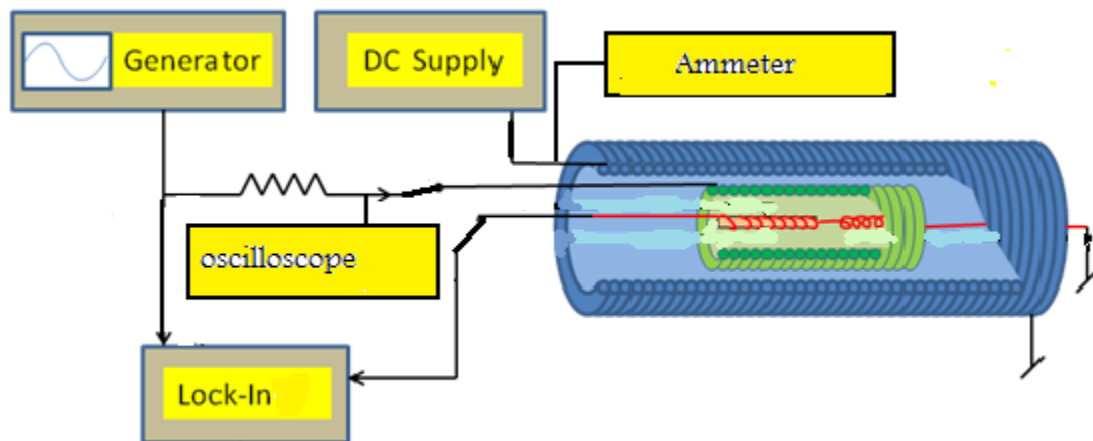


Figure 11: Resonance Test Configuration FeSiB

A signal was introduced to the driving coil at 20 kHz (non-resonant frequency) to produce changes of magnetization of the sample. This in turn generated a signal in the pickup coil from the changes in flux exclusive to that coil due to the compensating coil. From there the power source connected to the bias coil was turned on and set to maximum negative

setting that was able to be safely obtained. Due to heat generation by the coil and not wanting to cause other problems that a high current could present the current was kept to 1.5 amperes. A multimeter (working as ammeter) was also attached to be able to accurately monitor current. This knowledge can be used to check the direct current field generated by the bias coil. The field was then changed from the maximum negative field able to be generated for the first setting of the bias coil to maximum positive field that was able to be generated at the set parameters. Points were plotted from the signal registered on the lock-in amplifier from the pickup coil. The points were then taken and converted from the millivolts shown on the lock-in amplifier to induced magnetization then finally to relative permeability. This calculation process will be shown in the next test dealing with resonance and permeability. The following graph shows the relative permeability in relation to the magnetic bias field for a non-resonant frequency.

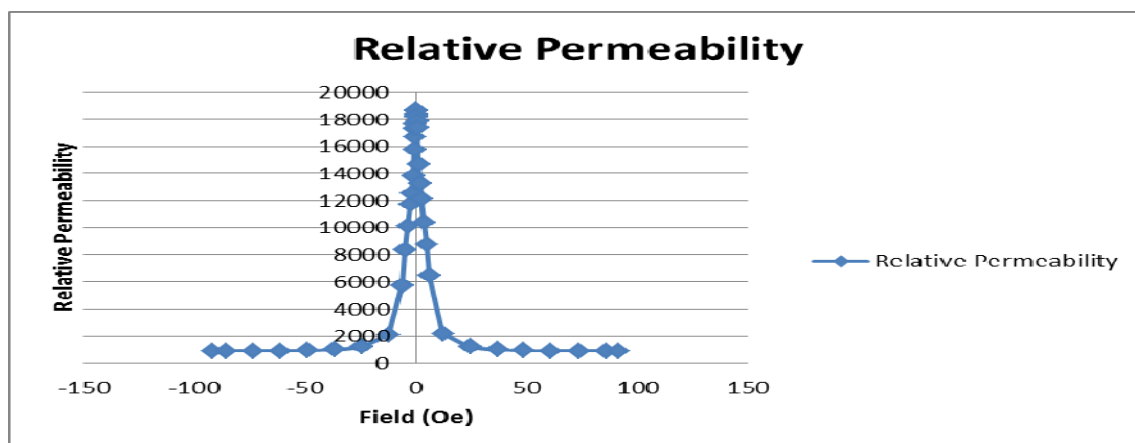


Figure 12: Relative permeability as a function of bias field for FeSiB/PZT

It should also be noted that the raw data recorded as the field was swept from negative to positive and back can be integrated to form a hysteresis loop and allow you to see the coercive field of the sample. Thus, being able to determine how magnetically soft your sample is. The prior graph shows the equation for the converse magnetoelectric effect equation (15) components set up as $\Delta B = \mu \Delta H$. Thus, allowing a purely magnetic measurement to be taken.

It is also believed that the system can be used to find a hysteresis loop for the electric material. This loop could be measured by increasing the voltage applied directly to the sample through attached leads. However, due to equipment constraints (insufficient voltage to overcome coercive field) we could not generate this loop. An example from literature shows what this loop may look like. The example chosen was from a paper written by R. Desfeux titled *Correlation between local hysteresis and crystallite orientation in PZT thin films deposited on Si and MgO substrates*. [10]

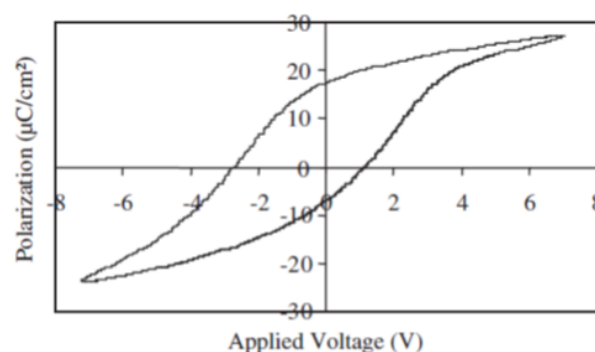


Figure 13: PZT Hysteresis loop from "Correlation between local hysteresis and crystallite orientation in PZT thin films deposited on Si and MgO Substrates."

Due to the thickness of the PZT ceramic plate used for this experiment we could not generate a large enough field safely to saturate the sample. However, for thinner samples this procedure could be used in addition to the ferroelectric tester available in AMRI labs. The graph above would represent a measurement of the equation $\Delta D = \epsilon \Delta E$ which would make it purely electrical using components of equation 14.

4.2 Magnetomechanical Resonance:

The system in Fig. 9 was arranged so that it could be used to measure magnetomechanical resonance, i.e. test how the relative permeability of the magnetic component varies with frequency near the magnetomechanical resonance. All three coils are present but the bias coil is off (or can be set to a fixed field). Only the driving coil has a signal passing through it. Then the pickup coil registers the change in flux due to the sample and transmits it to the lock-in amplifier. No leads going directly to the sample are being attached. With this configuration it is true that only the magnetic properties of the ribbon will be studied. This procedure will allow us to record the resonant frequency and start to perform calculations for the permeability of the sample. The following graph was a result of this frequency sweep. It shows the calculated permeability versus frequency.

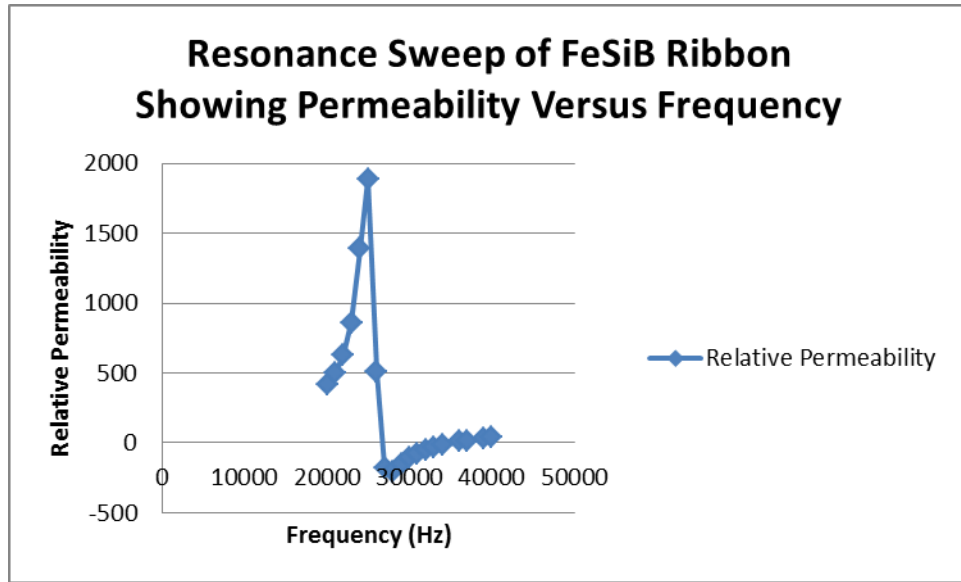


Figure 14: Resonance Sweep of FeSiB Amorphous Ribbon showing relative permeability versus Frequency

Using equations from previous sections a calculation of H , B and μ can now be done. Identifying that the only components used of the prior equations are listed in the previous sentence we set up our equation using components of equation 2 as such:

$$B = \mu H + qS \quad (15)$$

where S represents the strain generated by the resonant vibrations of the ferromagnetic component generated by ac magnetic field due to magnetostrictive properties of the metallic glass. This test takes into account qS in addition to magnetic permeability term μH of non-magnetostrictive sample.

From the raw data recorded the resonance frequency and measured signal can be obtained. This would be when the measured signal due to the

magnetic induction is greatest and the associated frequency will be the resonant frequency. Using a twenty-turn pick up coil, which is not a part of the system, a signal was measured to assist in the calculation of H. The cross-section of this coil was measured to be 0.000346 m^2 . With resonance being at 25 KHz and a measured signal from the separately fabricated pickup coil of 8.922 mV the equation can be set up with a few other known parameters to look like the following:

$$H = \frac{0.008454V}{(20) (.000346 \text{ m}^2)(2 \pi) (25000\text{Hz}) \mu_0} \quad (16)$$

Measured field generated by the driving coil inside the pickup coil equates to 6.1954 A/m. This is the amplitude of the ac magnetic field which produced the changes of magnetization of the magnetic layer of the composite sample.

Next, the measurements of length and width were taken to give a cross sectional area of the sample. This area equates to $7.10458 \times 10^{-8} \text{ m}^2$. Then knowing the pickup coil had 100 turns we use that as the first term of the denominator. From the graph in Figure 12 above we see that the frequency to use is 25 KHz which is also what the driving magnetic field was calculated at. The generated signal from the change in flux in the pickup coil due to the sample was recorded to be 0.01639 v. Using these measurements in the following equation magnetic induction can be calculated. The equation looks like the following with values plugged in:

$$B = \frac{.01639V}{(100) (7.10458 \times 10^{-8} m^2) (2 \pi) (25,000 Hz)} \quad (17)$$

Running the calculation it is found that $B = 1.469 \times 10^{-2} T$. Finally, given B and H a calculation for permeability can be done. Taking the equation mentioned at the beginning of $B = \mu H$ and plugging in the previously solved for results we can solve for μ . Once all components are plugged in the equation should look like $1.469 \times 10^{-2} T = \mu_r \mu_0 (6.19536 A/m)$. With manipulation of this equation it is found that the relative permeability of the sample μ_r is 1,888.

4.3 Electromechanical Resonance:

Then the configuration of the system was arranged to test the properties exclusive to the electric phase of the sample. This was done by attaching the leads from the sample to the function generator. A resistor was placed in series as well to measure the ac current from the capacitor structure. The lock-in amplifier was then connected to either side of the resistor allowing us to measure the induced electric field generated versus the frequency. All the magnetic coils were turned off for this experiment. The following schematic shows this set up. This setup can test electromechanical resonance by measuring the change of impedance of the capacitor structure when resonant vibrations of the piezoelectric component are caused by the alternating strains of the piezoelectric component.

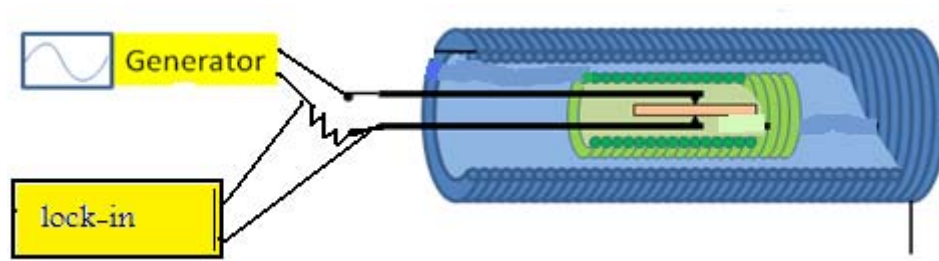


Figure 15: Configuration for exclusively electric data results

Thus the measurement only correlated to $D = \epsilon E + eS$ of the two sets of equations. This being the electric displacement equal to the permittivity multiplied with the electric field and coupled with the strain portion due to the interaction through the epoxy with the amorphous ribbon. The following two graphs show an electromechanical resonance and then the data was manipulated by subtracting out the slope of the line to enhance the resonance display in the second graph.

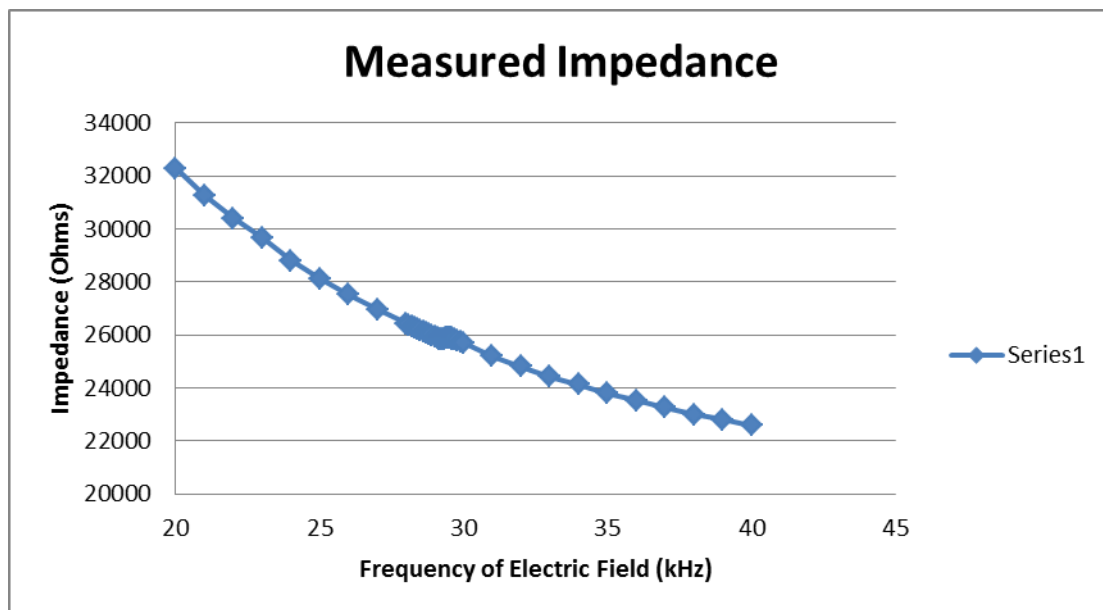


Figure 16: Electromechanical resonance sweep

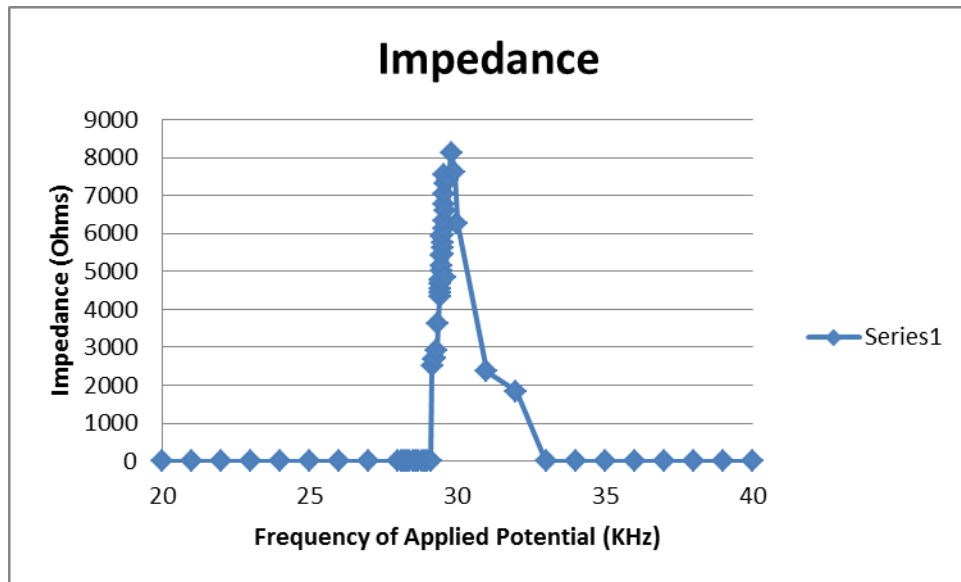


Figure 17: Measured Impedance with frequency dependence subtracted

This step shows you can measure electro mechanical resonance and also with known constants of your material such as permittivity calculate your electric displacement.

The previous experiments were run with exclusivity shown to either the magnetic portion of the sample or the electric portion. This system was designed to allow for those results but also to evaluate the coupling of the properties. The following procedures and results show how the system can generate data showing the coupling.

4.4 Magnetoelectric Effect- Direct:

In addition to the equation $B = d^T E + qS + \mu H$ being able to be tested it can be shown where the electric displacement depends on H in the equation $D =$

$\epsilon E + eS + \alpha H$. Here the eS and αH components were taken in to account to set up the equation $D = eS + \alpha H$. In the set up of the system the leads from the sample were attached to lock-in amplifier. The function generator was connected to the driving coil and the bias coil was connected to a power supply set to maximize the samples response. The function generator was then used to sweep of 10 Vpp across a frequency range of 20 KHz to 45 KHz. The system was set up as the following schematic indicates.

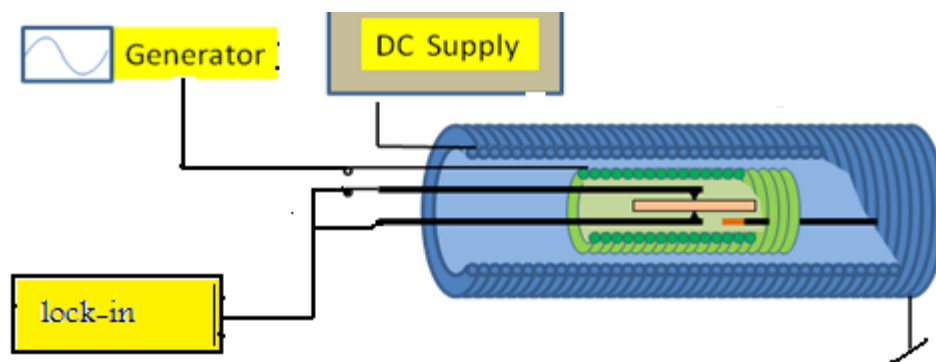


Figure 18: Schematic for electric displacement due to ΔH system connections

Data resulting from this test showed a measureable increase around the resonant point for the sample. The resultant signal was purely an electrical signal generated by the sample due to the changing applied alternating magnetic field. As can be seen in the following graph there was a definite signal change produced by the sample.

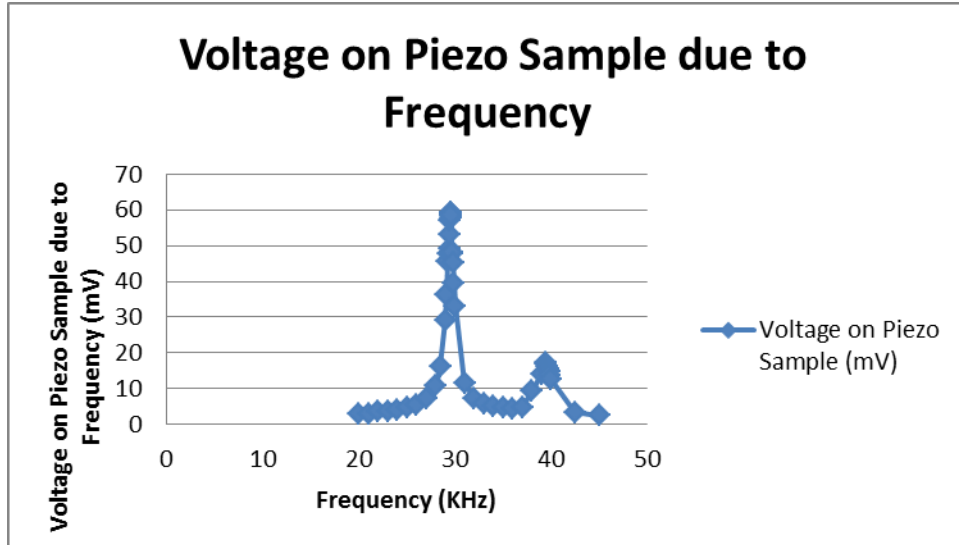


Figure 19: Magnetic field frequency versus changes in electric displacement signal

4.5 Magnetoelectric Effect – Converse:

Next step was reading the change in induced magnetization in relation to the change in the electric field. These next few experiments focus on using the entire $B = \alpha^T E + qS + \mu H$ equation for resonant frequency or the part $B = \alpha^T E + \mu H$ for nonresonant frequency of the ac magnetic field. By applying an alternating potential across the sample a scan was run for the resonant frequency. This was done by setting the bias coil to not have any bias to maximize the response. This information was taken from data collected in the prior sections. On the function generator channel one was attached to the driving coil at 20 KHz with the amplitude set to 10 volts peak to peak to excite vibrations of the sample. The sample was attached to the second channel on the function generator that could generate an independent

signal. This channel was set to produce a signal of $10V_{pp}$ and the range was scanned from 25 KHz to 35 KHz due to our resonance point being in that range. The signal was also passed through an amplifying power supply to allow extra electric bias to be applied to the sample. The following schematic shows the connections of the coils:

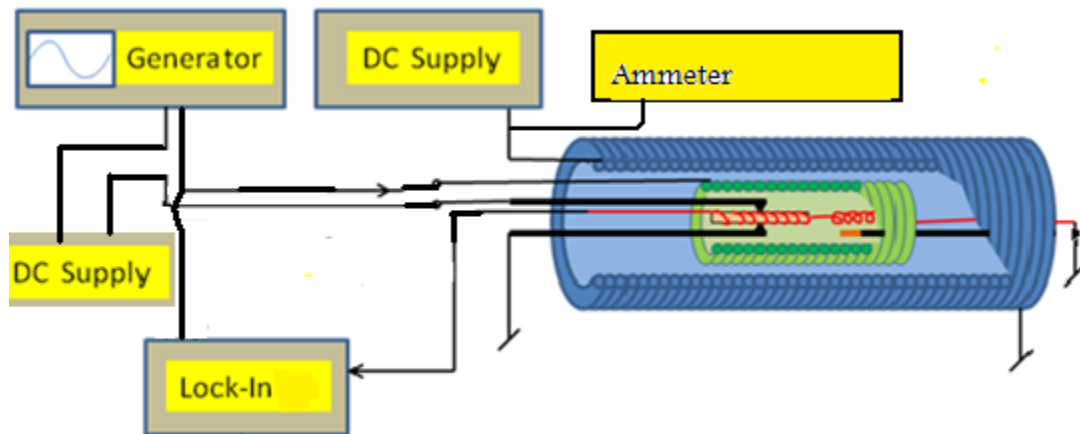


Figure 20: General configuration for electric resonance sweep

Once the system was properly connected the frequency was scanned for five different electric bias potentials. They were -40V, -20V, 0V, +20V, and +40V. The following graph shows the resonance peak shifting up and down with the applied bias to the sample. This is representative of the equation $B = a^T E + \mu H$.

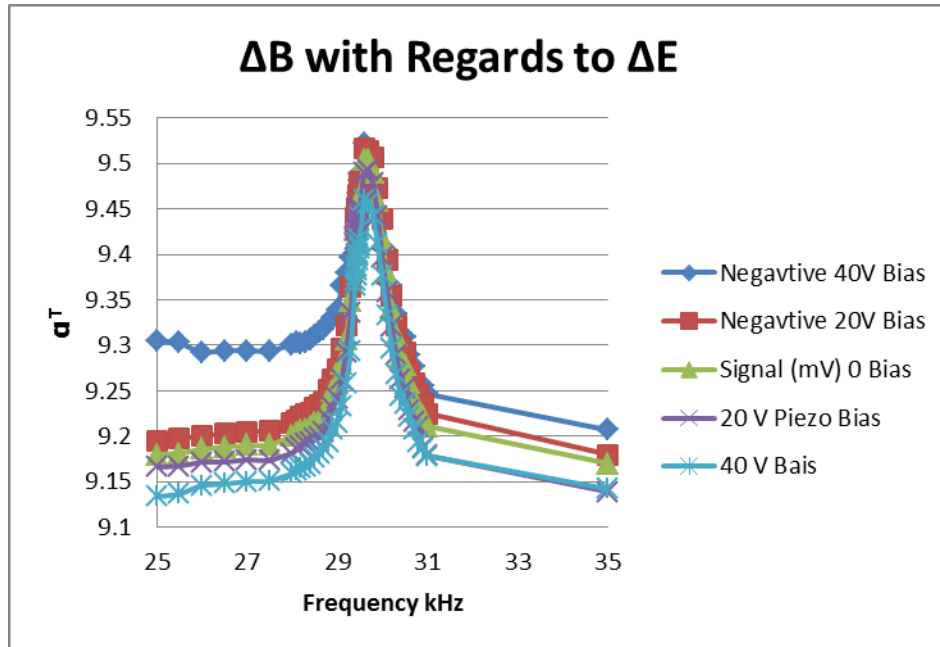


Figure 21: Resonance frequency scan for the applied E field of PZT showing α^T

It appears that the ac strains depend on the bias. Because of the magnetoelectric coupling they increase or decrease the amplitude of the signal and so the permeability. However, this extra term did not shift the resonant frequency. The graph shows how the induced magnetization measured by the pickup coil is coupled to the electric frequency applied across the sample. Thus, the electric component of the sample affects the magnetic sample and has a quantitative change.

Following the previous step is another test to see how the signal changes from just the magnetic component being at resonance to both facets of the sample vibrating at resonance. The sample was again attached to channel 2 of the function generator and the driving coil was connected to channel 1. A connection was made from the lock-in amplifier to the pickup coil. Channel

1 had its frequency tuned to the resonant signal for the sample of 29.5 KHz. Channel 2 was set to 20 KHz and swept through 50 KHz with amplitude of 10 volts from peak to peak. The bias coil was set to generate a 0.3 Oe bias field as this was the bias that showed maximum response allowed. Channel 1 was cycled on and off at each set frequency during the sweep to be able to determine how the effect was enhanced due to both the electrical and magnetic fields being on as opposed to just the electrical field driving the measured signal. The schematic looks the same as the previous one. However, different parameters were changed to generate the results. The experimental results show ΔB as a function of ΔE and also ΔB in relation to $\Delta E + \Delta H$. Thus the experiment uses $B = \alpha^T E + qS + \mu H$ (blue curve) and $B = \alpha^T E + qS$ (red curve in Fig. 22).

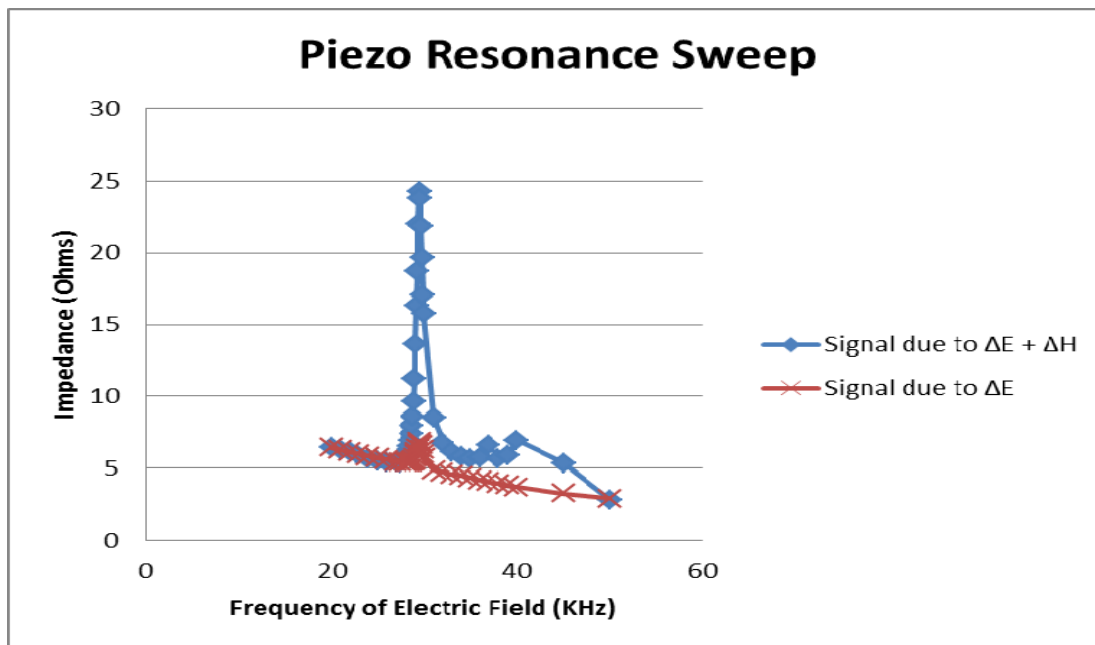


Figure 22: Measured change in B comparison due to E and frequency

The graph above shows the response of the sample is greatly enhanced due to both the magnetic and electrical portions of the sample being excited simultaneously.

In the ensuing experiment we take the magnetic signal alone in a bias field sweep then couple it with the electric field component to observe how the induced magnetization of the pickup coil changes. This was set up to having both channels set to the resonant frequency. Once the reading was taken for both channels being on channel one would be turned off and a second reading taken so that a comparison of the two signals could be made to show any enhancements both signals being on versus one being on could achieve. Again this is a measurement using the principles established in the equation $B = \alpha^T E + qS + \mu H$ (blue symbols) and the isolated case of $B = qS + \mu H$ (red symb. in fig. 22) in comparison. The following graph is the result:

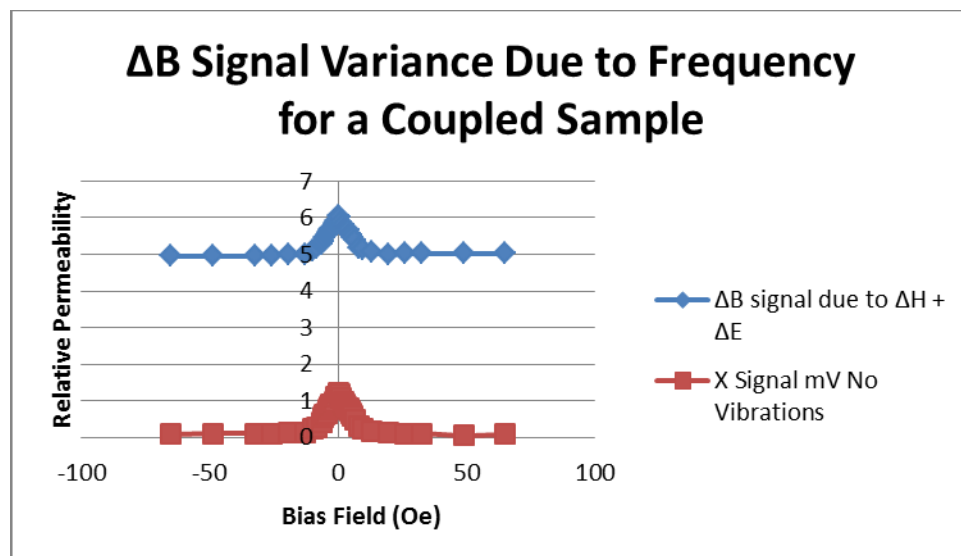


Figure 23: Signal varying due to bias field sweeps

As can be seen the signal related to ΔB is greatly enhanced by the electric field.

Finally, an experiment was run to see what the actual ratio was of the sample being at resonance at various applied amplitudes for a coupled signal versus the magnetic resonant signal alone. There were various amplitudes applied from the generator to see where the effect could be seen most clearly. This was done by taking the readings with driving coil always having an applied signal from the function generator. The second channel was cycled between on and off. After each cycle the amplitude of the applied signal to the driving coil was reduced. After all the data was collected a calculation was done and graphed. The equation was:

$$\frac{V_P - V_Q}{V_Q} \quad (18)$$

This establishes a ratio for where the response is greatest relative to the conditions. As can be seen in the following graph multiple amplitudes were recorded with both signals on then just the driving coils signal measured.

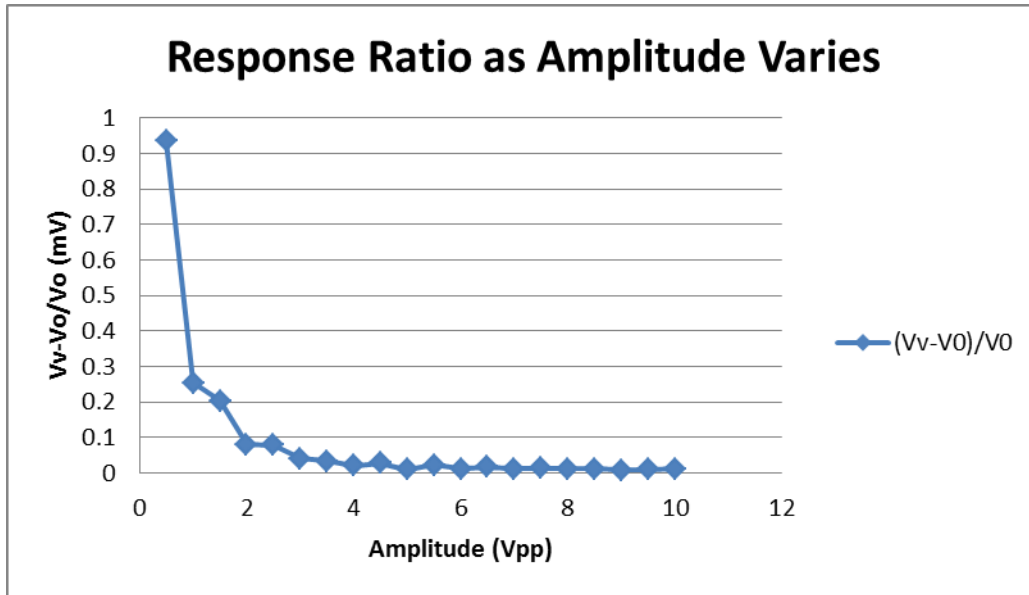


Figure 24: Ratio of response as a result of amplitude variation.

This graph shows that at lower amplitudes the response of the sample to both fields nearly doubles the response of the magnetically induced signal. As the amplitude increases the signal difference reduces to a difference of only a few percentage points. This is good knowledge to have when testing samples with hopes of achieving results for both the magnetoelectric and converse magnetoelectric effect.

Chapter 5

Conclusions

The first sample of $\text{Fe}_{78}\text{Si}_{10}\text{B}_{10}/\text{AlN}$ made it possible for a signal to be recorded which proved that it is possible to measure different resonances of a vibrating composite sample (bending or longitudinal) due to the ac magnetic field excitation. These measurements can be used to characterize the samples magnetic qualities. Relative permeability can be calculated from the resultant data. This also displays magneto mechanical resonance for the given sample.

The second sample of $\text{Fe}_{78}\text{Si}_{10}\text{B}_{12}/\text{PZT}$ proved that the system works in its entirety. First, there were data points collected that could be plotted to form a non-integrated hysteresis loop. This could also be portrayed in terms of relative permeability versus bias field. Thus, this system could be used to find the coercive field of a sample and determine how magnetically soft it is. It was determined for thin samples an electric hysteresis loop could also be charted. However, for the sample that was used in relation to samples recorded in literature a field of megavolts was required and could not be obtained.

Next, the system was successful in finding the resonance of the sample. By adjusting the driving magnetic field H by sweeping a frequency range a

resonance peak appeared. Using known measured factors of the driving field, pickup coil, measured signal generated by the sample and some constants it was possible to calculate the relative permeability of the sample. This result showed the system was able to measure for the equations $B = qS + \mu H$ governing the magnetomechanical resonance. This relation could also be tested in the composite laminate sample.

With a variation in the connections made in the system it was possible to measure an electrically exclusive property. This allows the $D = \epsilon E + eS$ equation to be tested. A clear electromechanical resonance peak can be seen due to the change in the frequency of the applied electric field. This measurement proves that the piezoelectric plate can be tested for characterizing properties.

Following the magnetic and electric properties of the sample that could be isolated, the sample could be tested for coupled properties. Meaning, the sample could have an applied electrical field and have a measurable magnetic property register. Conversely, a change in the magnetic field applied could register a measurable change in an electric property.

In this line of thought the system was set up to show a measurement relating to $B = \alpha^T E + qS$ where the electric signal applied to the sample had the frequency scanned from 20 KHz to 40 KHz and a resonance peak showed up in the measured response relating to ΔB . Also, the enhanced response

can be seen when both signals, magnetic and electric, are at resonance. When a bias field sweep was done for the just the magnetic signal and then both signals being applied there is a prominent enhancement in the amplitude of the signal. This proves that the fabricated system is capable of measuring the coupling between the electrical and magnetic components of a multiferroic sample by electric components influencing the magnetic measurements.

Measuring the change in electric properties due to a variance in the applied magnetic components was also observed. The equation $D = qS + \alpha H$ would be the relation shown by the configuration. This was achieved by connecting the sample to the lock-in and sweeping a frequency range of signal applied to the driving coil. Thus the electric properties changed in relation to the variance of the alternating magnetic field.

Finally, the ability to measure the responses individually and as a combination in a method to determine at which settings they are maximized was achieved. By incrementally stepping down the amplitude of the applied magnetic field it was possible to see the difference in response was the greatest at lower amplitudes. When at the lowest amplitude measured the difference between magnetic response and joint response was almost two fold. Where at larger amplitudes it was only a one to two percent change. This is believed to nonlinear properties of the system and saturation of magnetization at larger stress amplitudes.

In conclusion this system was successful in measuring components of both equations both isolated and coupled. The initial test showed that the magnetic and electric properties of multiferroic composites are mutually coupled and their complex relations can be established as functions of frequency of applied magnetic or electric fields, their amplitudes and electric and magnetic bias. The system can be further developed to include automatic data acquisition. Specific procedures for evaluation of magnetoelectric parameters from the measurements can be devised and variety of magnetoelectric materials tested. These tasks were beyond the scope of the thesis.

Table 1: Lists of possible measurements in the system

Equation	Measuring Conditions		Properties Measured
	Signals applied	Signal measured	
$B = \mu H$	AC coil on, DC sweep signal in	AC voltage on pick-up coil (permeability)	Permeability, coercivity, saturation magnetic field
$D = \epsilon E$	AC voltage on PZT	AC current on the PZT	Permittivity, coercivity, saturation electric field
$B = \mu H + qS$	AC coil on frequency sweep	Voltage on a coil	Magnetomechanical coupling
$D = \epsilon E + eS$	AC voltage on PZT, frequency sweep	AC current from PZT (impedance)	Electromechanical coupling

Table 1A: Table of possible measurements

$D = \alpha H$	AC coil on	AC voltage on PZT	Magnetoelectric coefficient
$B = \alpha^* E$	AC voltage on PZT	Pick-up coil on	Converse magnetoelectric coefficient
$D = \epsilon E + eS + \alpha H$	A voltage on PZT and AC coil on, DC bias on	Current on PZT	Mutual relations between B and D
$B = \mu H + qS + \alpha^* E$	A voltage on PZT and AC coil on DC Bias on	Pick-up coil on	Mutual relations between B and D

Table 2B: Table of possible measurements continued

References

- [1] Cullity, B.D. and Graham, C.D. Introduction to Magnetic Materials. New York: John Wiley and Sons, 2009. 241.
- [2] Cullity, B.D. and Graham, C.D. Introduction to Magnetic Materials. New York: John Wiley and Sons, 2009. 257.
- [3] Cullity, B.D. and Graham, C.D. Introduction to Magnetic Materials. New York: John Wiley and Sons, 2009. 243.
- [4] Luo, Hongyu. "Colloidal Processing of PMN-PT Thick Films for Piezoelectric Sensor Applications" Diss. Drexel University, 2005.
- [5] Wangsness, Roald. Electromagnetic Fields. New York: John Wiley and Sons, 1986.
- [6] Piezo Systems Inc. Catalog 8. 2011. 59-61.
- [7] Halliday, David, Resnick, Robert, and Walker, Jearl. Fundamentals of Physics. Vol. 1. New York: John Wiley and Sons, 2001. 390.
- [8] Thornton, Stephen, and Marion, Jerry. Classical Dynamics of Particles and Systems. California: Brooks/Cole-Thomson Learning, 2004.
- [9] Taylor, John. Classical Mechanics. California: University Science Books, 2005. 187.
- [10] Taylor, John. Classical Mechanics. California: University Science Books, 2005. 189-190.
- [11] Squire, P.T. "Magnetomechanical Measurements of Magnetically Soft Amorphous Materials." Measurement Science and Technology. 5 (1993) 67-81.
- [12] Fiebig, Manfred. "Revival of the magnetoelectric effect." Journal of Physics D: Applied Physics (2005) R123.
- [13] Wang, Yaojin et al. "PMN-PT single crystal and Terfenol-D alloy magnetoelectric laminated composites for electromagnetic device applications." Journal of the Ceramic Society of Japan (2008) 540

- [14] Fiebig, Manfred. "Revival of the magnetoelectric effect." Journal of Physics D: Applied Physics (2005) R124.
- [15] Wang, Yaojin et al. "PMN-PT single crystal and Terfenol-D alloy magnetoelectric laminated composites for electromagnetic device applications." Journal of the Ceramic Society of Japan (2008) 541.
- [16] Nan, Ce-Wen et al. "Multiferroic magnetoelectric composites: Historical perspective, status, and future directions." JOURNAL OF APPLIED PHYSICS 103 (2008) 031101-4.
- [17] Department of Physics. University of Arizona. Physics 241 Lab: Solenoids. 2011.
- [18] Department of Physics and Astronomy. Georgia State University. Ampere's Law. < <http://hyperphysics.phy-astr.gsu.edu/hbase/magnetic/amplaw.html>>

Vita

Thomas Ward IV was born in Eden, North Carolina July 5, 1985. He attended Roanoke College in Salem, Virginia and earned a Bachelor of Science in Physics in May 2007. After that he went to work for Balzer Engineering before joining Dr. Malkinski's group to pursue a MS in Applied Physics. Currently works for Gallo Mechanical as an estimator.